

Vilnius University  
Faculty of Physics

Theodore Ngalle Etoke

"ELECTRICAL PROPERTIES OF NANO CRYSTALLIZED GLASSY CATHODE MATERIALS"  
by  
impedance spectroscopy experiments.

Master's practical research work  
Electronics and telecommunication engineering

Student

Theodore Ngalle Etoke

Academic supervisor

doc. Edvardas Kazakevičius

Director/ representative of the Institute / Center

prof. Robertas Grigalaitis

Vilnius 2023

# Contents

1. INTRODUCTION .....	3
2. LITERATURE REVIEW .....	4
3. IMPEDANCE SPECTROSCOPY .....	5
3.1 EXPERIMENTAL .....	9
4. METHOD1: EQUIVALENT CIRCUIT .....	11
6.1 CONDUCTIVITY .....	14
4. METHOD2: DRT ANALYSIS .....	16
5. GAUSSIAN FIT OF DRT .....	18
5.1 MULTYPEAK FITTING OF DRT .....	18
5.2 FITTING IMPEDANCE SPECTRA IN Zview.....	20
CONCLUSION .....	22
SUMMARY .....	23
APPENDIX: DISTRIBUTED ELEMENT(DE) .....	26

# 1. INTRODUCTION

Long ago renewable energy sources play an important role in the global energy transition. Their operations depend on the atmospheric condition as such they are known as AC power. To meet the demand in the network, it is, therefore, necessary to store and use surpluses during a period of scarcity. Lithium-ion batteries are used in portable electronic devices and electric vehicles. Their main advantages are an operating voltage of 3.2 to 4.0 V and an energy density of up to 250 Wh/kg. Scientists are struggling to find a cheap/widely available alternative to lithium. One of these can be sodium, which is also an alkali metal. Sodium batteries usually have a lower capacity and a lower operating voltage. Despite this, the energy density is still quite high, making them good candidates for long-term and economical large-scale energy storage [1]. For the battery, we need an electrode with mixed conductivity nanostructure. Nanostructured glass-ceramic materials with significantly improved electrical conductivity (ionic or electronic) or an extended temperature stability range of highly conductive high-temperature crystalline phases. Such materials have been synthesized by thermal nanocrystallization of selected electrically conductive oxide glasses [2]. An effective method for obtaining nanostructured material is the thermal nanocrystallization of glasses. These kind of materials has already found many practical applications in fiber optic devices, heat-resistant materials, hard disk substrates, dental materials, and many others [3]. The key to performance in a wide range of applications is the transportation of mobile ions in ionic conductors, including portable power supplies with primary and secondary batteries, chemical sensors, power generators, fuel cells, instrument electronics, and electric vehicle technology.

This research work aims to investigate experimentally the dynamic response of mobile ions in NASICON base glass ( $\text{Na}_3\text{VTi}(\text{PO}_4)_2\text{F}_3$ ) during the crystallization. The impedance spectroscopy (IS) was used for the purpose. It is based on the interaction of the electric charge of the species inside the sample with an applied electric field and measuring the magnitude of this interaction and its properties over a period of 17 hours.

## 2. LITERATURE REVIEW

### NASICON-LIKE PHOSPHATE GLASSES

The acronym NASICON (NAtrium-SuperIonic-CONductor) was given to fast Na<sup>+</sup> ionic conductors eg Na<sub>3</sub>Ti(PO<sub>4</sub>)<sub>3</sub> which do not conduct electrons. These compounds are a class of structurally isomorphic 3D framework compounds with high ionic conductivity, often comparable to those of liquid electrolytes at higher temperatures. This unique property gives the possibility to synthesize compounds that exhibit mixed *electronic-ionic* conductivity, for example, Na<sub>3</sub>VTi(PO<sub>4</sub>)<sub>2</sub>F<sub>3</sub>. Therefore, materials of this family can be used in both cathodes and electrolytes in Na-ion batteries. Thus, the concept of NASICON solid-state electrochemical cells was born. In this approach, a sodium-ion battery could be composed of NASICON-type mixed (electronic ionic) conductors as a cathode and an anode, and a "traditional" ionic conductor as an electrolyte/separator. Na<sub>3</sub>V<sub>2</sub>(PO<sub>4</sub>)<sub>3</sub> and Na<sub>3</sub>V<sub>2</sub>(PO<sub>4</sub>)<sub>2</sub>F<sub>3</sub> with the NASICON structure are among the most promising materials for the Na-ion battery cathodes. A replacement of one phosphate group by three fluorine ions results in a compound with a tetragonal structure[4] and can be extra beneficial for several reasons: First, it decreases the molar mass of the compound, increasing theoretical gravimetric capacity; Second, it increases the electrochemical potential versus metallic sodium; Third, it can introduce a more ionic character of sodium bonds and thereby increase mobility. Na<sub>3</sub>V<sub>2</sub>(PO<sub>4</sub>)<sub>2</sub>F<sub>3</sub> with a tetragonal structure shows rich chemistry and attractive lithium/sodium insertion properties and therefore offers promising electrochemical properties. It was prior reported by Meins [5] to have a space group of P42/nm for materials synthesized by solid-state sintering. As of now, the interest in Na<sub>3</sub>V<sub>2</sub>(PO<sub>4</sub>)<sub>2</sub>F<sub>3</sub> (or isostructural) polycrystalline cathode materials has increased significantly, leading to many scientific papers.

### 3. IMPEDANCE SPECTROSCOPY

Impedance spectroscopy (IS) is a powerful technique used in applications such as electrochemistry, materials science, biology and medicine, the semiconductor industry, and sensors[6]. To date, this is the most commonly used method for experimental investigation of the dynamic response of mobile ions in ionic conductors which makes this method an ideal tool for studying the dynamics of particles with an electric charge in materials[6]. It is based on the interaction of the electric charge of particles inside the sample with an applied electric field and essentially consists in measuring the magnitude of this interaction and its characteristic frequency or time scale. We will pay more attention to the use of IS and its application to the measurement of the electric response of ionically conducting materials.

The electrical properties of materials have been characterized for many years using Impedance spectroscopy(IS). Due to its widespread use, scientists have made more efforts to improve it. The most common experimental setup allows to determine the impedance of the test sample by applying a sinusoidal (alternating) voltage (current) signal with known amplitude and frequency, as well as measured amplitude and phase shift. Assuming a linear characteristic, if a sinusoidal time-dependent voltage  $V(t)=V_0\sin (wt)$  is applied, the current will be a sinusoidal signal with the same frequency, but phase-shifted,  $I(t)=I_0\sin (wt-\phi t)$ . The angular frequency  $\omega$  (measured in rad/s) is related to the frequency  $f$  (in Hz) by the ratio  $\omega=2\pi f$ . (see figure 1)[14]

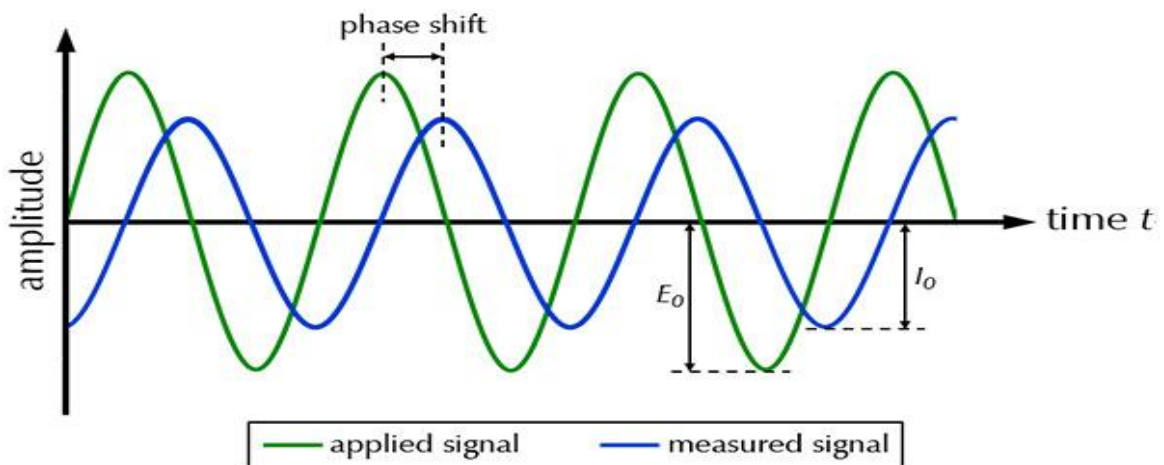


Figure 1: Current response to a sinusoidal voltage excitation in a linear system

In the time domain, the analysis of the periodic excitation by current or voltage is very complex. It requires solutions to differential equations. In this case, the use of the Fourier transform of the signal to the time domain helps simplify the problem. Using the ratio:

$$e^{i\omega t} = \cos(\omega t) + i\sin(\omega t) \quad (1)$$

The impedance can be expressed as a complex function of frequency. The voltage is the real part of the complex function (equation 1),

$$V = V_0 e^{i\omega t} \quad (a)$$

and similarly, the current is the real part

$$I = I_0 e^{i(\omega t - \phi)} \quad (b)$$

The impedance is defined as a complex function

$$Z = \frac{V}{I} = Z_0 e^{i\phi} = Z_0 \cos \phi + iZ_0 \sin \phi \quad (2)$$

linearity, causality, and stationarity of the system is the only condition that the Fourier transform can reduce a differential equation to algebraic equations[7].

We can represent the impedance

$$Z = Z' + iZ'' \quad (2a)$$

as a vector on the complex plane (Figure 2) with rectangular coordinates

$$Z' = Z_0 \cos \phi \quad \& \quad Z'' = Z_0 \sin \phi \quad (2b)$$

Equation (2) is the real and imaginary parts of the impedance. Impedance is the function of the frequency and the polar coordinates of the impedance can be expressed as its phase[8].

$$\phi = \tan^{-1}\left(\frac{Z''}{Z'}\right) \quad (2c)$$

$$|Z| = Z_0 = [(Z')^2 + (Z'')^2]^{\frac{1}{2}} \quad (2d)$$

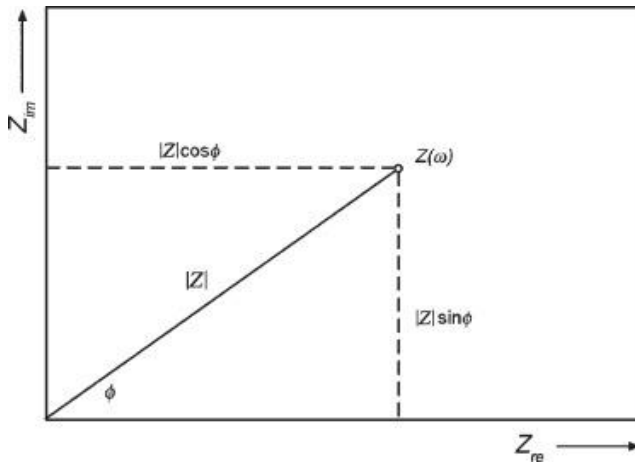


Figure 2: Impedance  $Z$  in the complex plane[14]

The IS consists in determining the frequency dependence of  $Z(\omega)$  by measuring its value for different frequencies in a given experimental frequency range. It is by this frequency dependence of the impedance that we could characterize the physical (or chemical) properties of the material or the interface of the material-electrode.

Impedance Spectroscopy (IS) allows us to measure the complex impedance  $Z$  of the available sample, as well as any other immittance function such as the complex admittance

$$Y=Z^{-1} \quad (i)$$

the complex capacitance

$$C^* = \frac{Y}{i\omega} \quad (ii)$$

and from them, by using a geometrical factor  $C_0$ , one can determine the dielectric permittivity

$$\epsilon^* = \frac{C^*}{C_0} \quad (iii)$$

the complex conductivity

$$\sigma^* = i\omega\varepsilon^* \quad (\text{iv})$$

$$\text{the electric modulus } M^* = \frac{1}{\varepsilon^*} C \quad (\text{v})$$

From the table, we can relate several impedance functions and correlate the relation between them.

*Table 3: Tabular relationships between several impedance functions*

	Z	Y	$\delta^*$	$\varepsilon^*$	$M^*$
Z=	-	$Y^{-1}$	$(C_0 \delta^*)^{-1}$	$(i\omega C_0 \varepsilon^*)^{-1}$	$M^*/ i\omega C_0$
Y=	$Z^{-1}$	-	$C_0 \delta^*$	$i\omega C_0 \varepsilon^*$	$i\omega C_0 / M^*$
$\delta$	$Z^{-1}/C_0$	$Y/ C_0$	-	$i\omega\varepsilon^*$	$I\omega/ M^*$
$\varepsilon=$	$Z^{-1}/i\omega C_0$	$Y/i\omega C_0$	$\delta/i\omega$	-	$(M^*)^{-1}$
$M^*$	$i\omega C_0 Z$	$i\omega C_0/Y$	$i\omega / \delta^*$	$(\varepsilon^*)^{-1}$	-



### 3.1 EXPERIMENTAL

This material ( $\text{Na}_3\text{VTi}(\text{PO}_4)_2\text{F}_3$  glass) is held in position with the electrode. The spectrometer provides the electric field through the material and is heated at a high temperature to nanocrystallise. For nanocrystallization we use temp(466.85 degrees Celcius) 740K, we maintain this temperature for 17 hours and we use  $\text{Na}_3\text{VTi}(\text{PO}_4)_2\text{F}_3$  glass as initial sample. During this time nanocrystallization was happening and we were measuring every half an hour impedance of the material, This process is called **in-situ**. The data was collected(33 points) and every half an hour and a Bode and Nyquist plot were drawn we see that they are quite complicated and we can obtain 3 responses, which are at high(1), middle(2), and low(3) frequencies respectively.

From Figure 4, we can see that we neglected the two other peaks(middle(2) and low(3) frequency) respectively, and considered only the highest frequency(broad peak). We try to analyze this broad peak, by assuming that the other peaks (2,3 and  $1^b = 1.98806$ , respectively) do not or have a small effect on the far away chosen section( $1^a = 0.3527$ ). The values 1.98806 and 0.3527 are coordinates of the selected portion to be investigated. We take this small portion  $1^a = 0.3527$  which is far away as possible in the highest frequency side of the peak from the other side and draw an equivalent circuit which is done using the software called Zview. We take the most simple circuit which is R and CPE(not ideal capacitor)

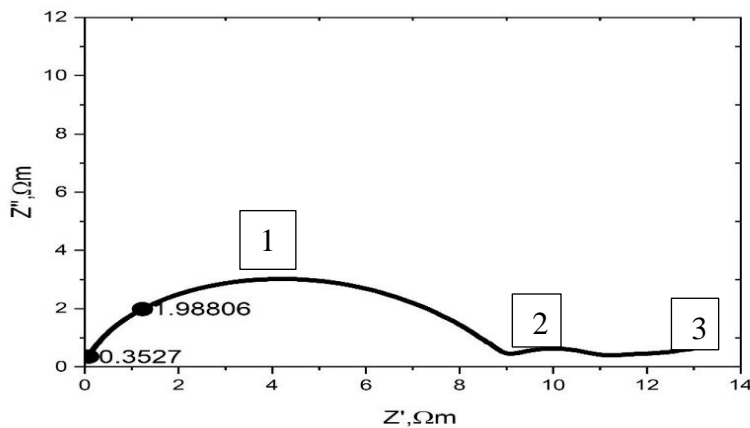


Figure 4: selected range far away from the other points

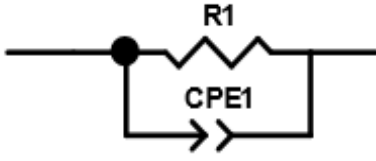


Figure 5: Equivalent circuit for the selected range on the Nyquist plot

Another way to analyze the result of electrochemical impedance spectroscopy data other than using the equivalent circuit is using the distribution of relaxation time (DRT) method. The well-known equivalent circuit method could be used for the analysis [9], but in some cases, the calculation of the so-called distribution function of relaxation times (DRT) yields better resolution [10]. The Namely DRT method will be used in this work. The method implies that the impedance spectrum of a conductive system can be presented as a sum of elements with individual relaxation times expressed by Fredholm integral equation of the first kind:

$$\tilde{z}(\omega) = \int_{-\infty}^{+\infty} f(\tau) \frac{1-i\omega\tau}{1+\omega^2\tau^2} d\ln(\tau) \quad (6)$$

Where  $z_{\infty}$  - high frequency limit impedance, ( $z_{\infty} \rightarrow 0$  in the case of sufficiently broadband data),  $f(\tau) > 0$  is the DRT function to be found,  $\tau$  - relaxation time,  $i$  - imaginary unit. The solution of Eq. (6) is known as an ill-posed problem but still,  $f(\tau)$  can be numerically found with a system of linear equations.

We used Python app for calculating the DRT. Its options panel allows users to import EIS data and select DRT calculation settings. The application was optimized for relaxation processes in solid electrolytes and this app is capable of finding nonparametric DRT by the Tikhonov regularization method. In principle, it is difficult to determine from Nyquist or Bode plots if two or more processes are overlapping or is just a single broad process. The main options of this tool include discretization methods, inductive data processing, data computation component, regularization parameter. This option of this tool allows us to measure the dynamics of different phases.

## 4. METHOD1: EQUIVALENT CIRCUIT

### RESULTS AND DISCUSSION

From the figures below which is at the beginning of the glass phase (heat-treat period), looking at the Bode and Nyquist plot, it was just one process which was noticed by the overlapping of the (fit) red and black plot (Figure 8) and this process lasted for 1 (one) hour and was later assumed to change into two semicircles with time.

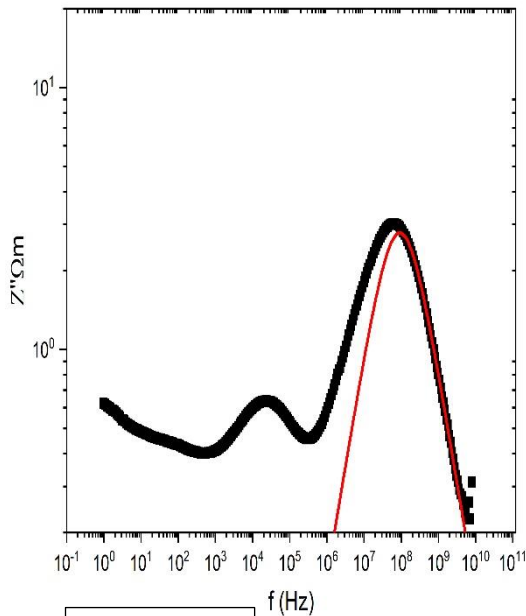


Figure 6

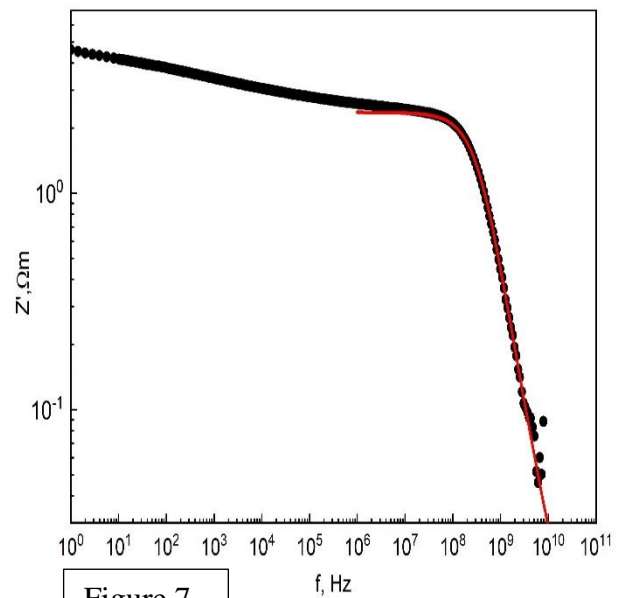


Figure 7

Figure 6&7: Bode plot of impedance spectra measurement and the fit of the selected region after 1 hour of heat treatment.

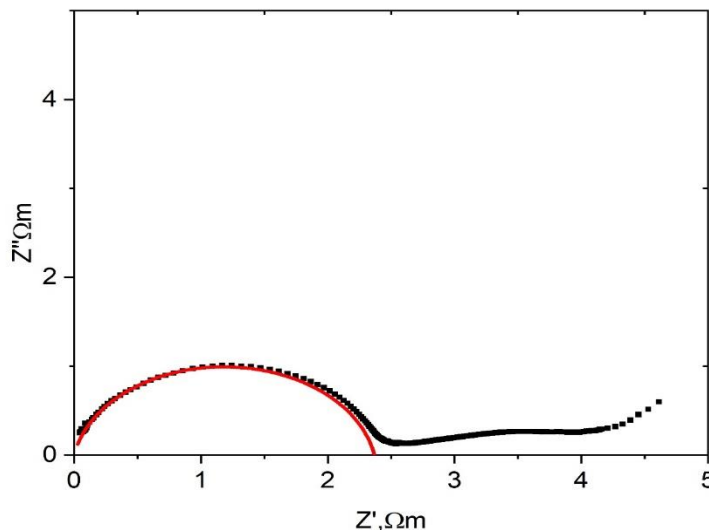


Figure 8: The Nyquist plot of impedance spectra within an hour of measurement

In the second phase after 4.4 hours of Looking at the Nyquist plot(Figure 11), we can see that the high frequency is overlapping, we assume it contains two processes that are not so clear on the bode plot(Figure 9&10) according to the deformation of the semicircle.

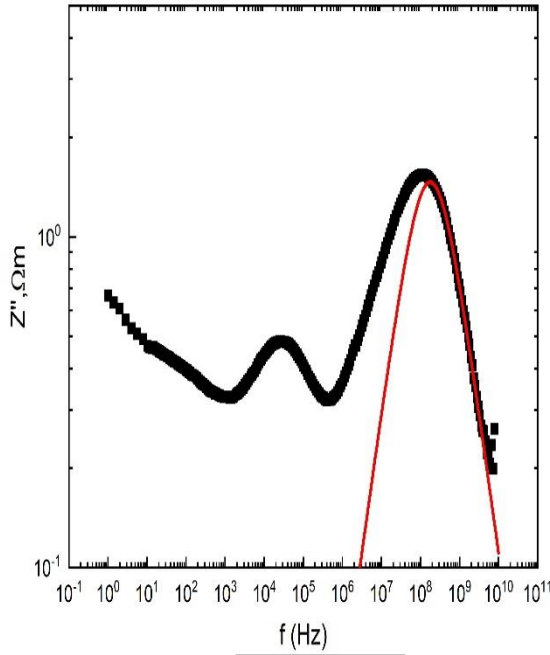


Figure 9

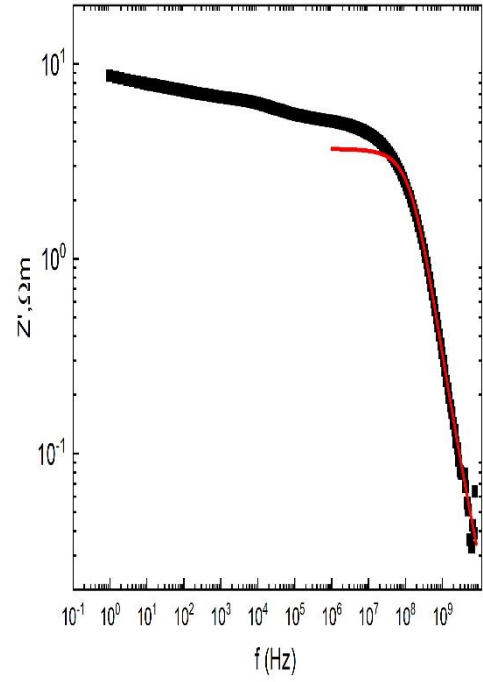


Figure 10

Figure 9&10: Bode plot of impedance spectra measurement and the fit of the selected region after 4 hours of heat treatment.

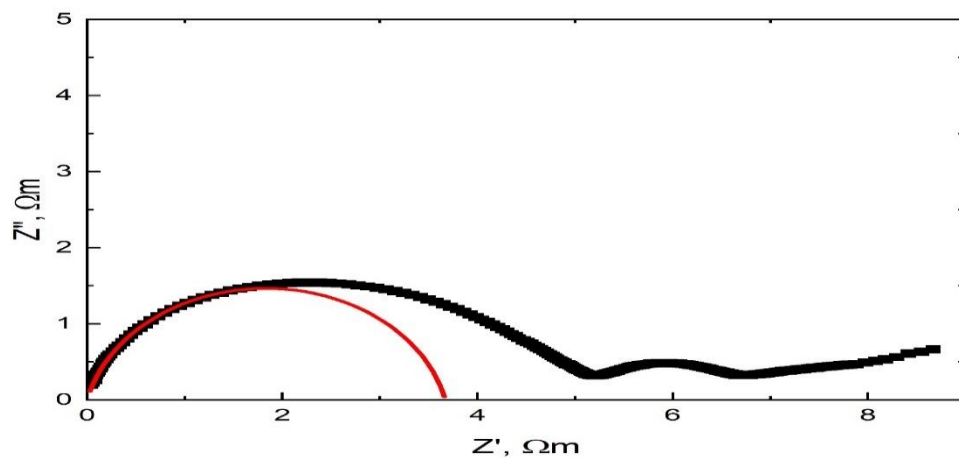


Figure 11: The Nyquist plot of impedance spectra within 4 hours of measurement

In the third phase(crystallized phase) which is at the end of the heat treatment, the body and the Nyquist plot seem to stay the same and this process began at the 8 hour.

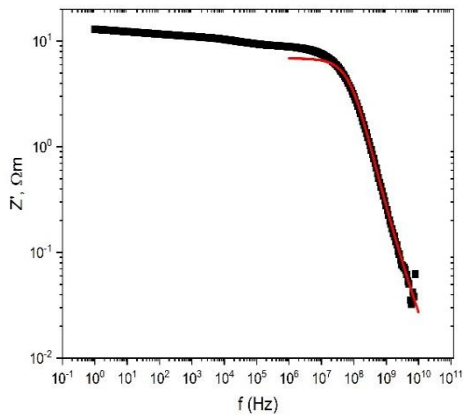


Figure 12

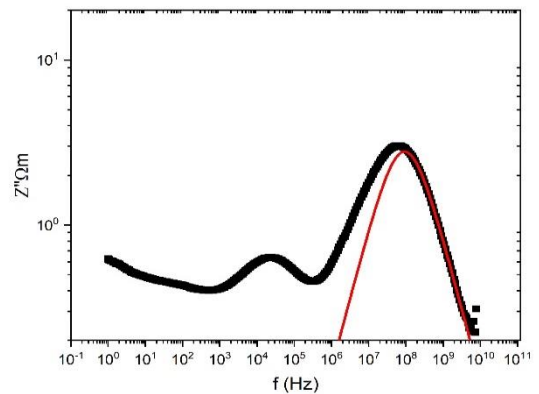


Figure13

Figure 12&13: Bode plot of impedance spectra measurement and the fit of the selected region after 8 hours heat treatment.

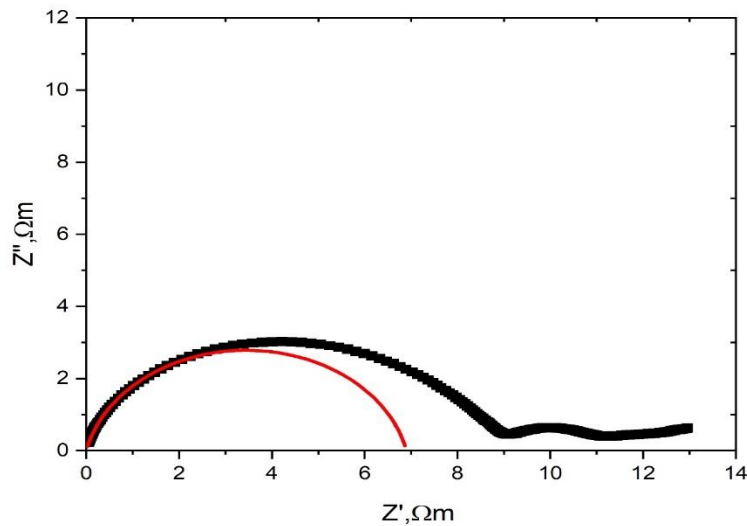


Figure 14: Nyquist plot of the impedance spectra after the heat treatment after 8 hours

$$f = \frac{1}{2\pi(RQ)^{1/n}} \quad [6]$$

Q= CPE coefficient,

f=frequency,

R= resistance

The equation above represents the relationship between the frequency and resistance of the impedance spectra.

## 6.1 CONDUCTIVITY

This calculation is done for the 33 points throughout the process (first, second and third phase) and the conductivity is calculated ( $\sigma(t) = 1/R$ ). After calculating the conductivity and data collected, a graph of conductivity against time is drawn.

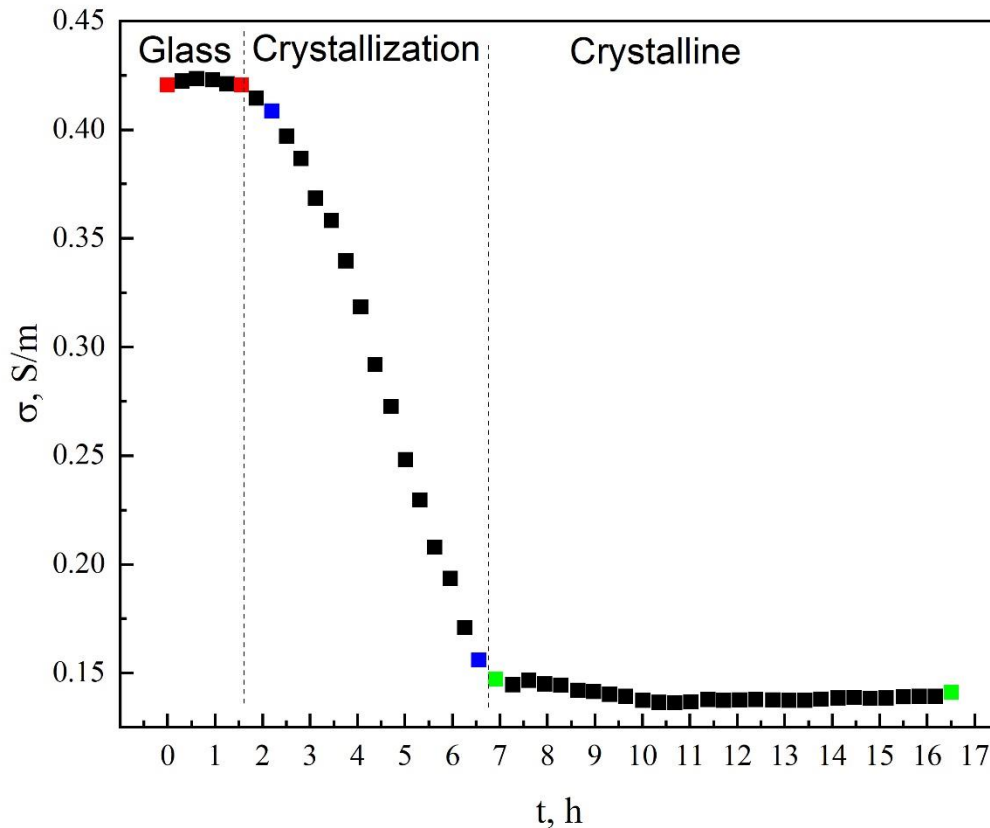


Figure 15: Conductivity dependent on time during heat treatment at 740k

From the graph of Figure 15, from the red point, we assume that the glass begins to nanocrystalize with time, and at the point with blue, the material takes some time to nanocrystalize and at the point with green, it is assumed that the process stops and remain unchanged. The conductivity the glass phase is roughly five times higher than the one of the crystalline phase.

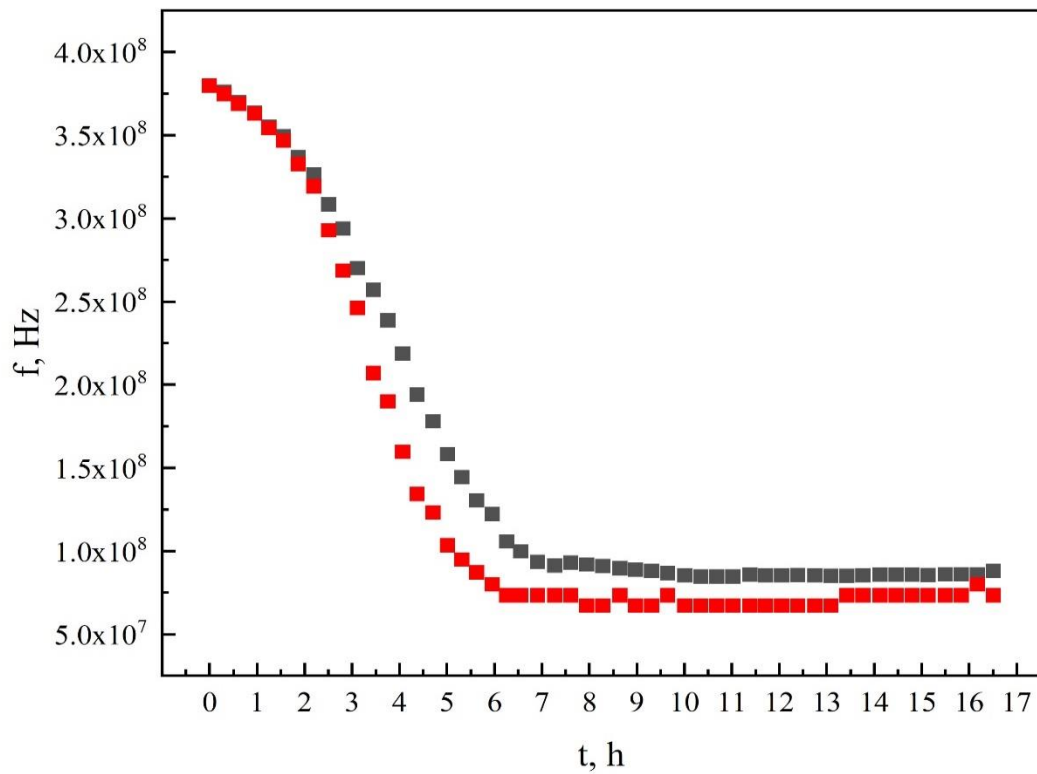


Figure 16: Representation of the frequency maxima and time(hour)

From figure 16, the graph of characteristic frequency and time, the red plot represents the **maxima** of the broad peak and the spectra and the black represents the fit of the equivalent circuit(see figure 9 to 11). In the beginning, it was just one process as this is confirmed by the overlapping of the red and black graph, they start to differ and power our assumption that two processes start to appear.

## 4. METHOD2: DRT ANALYSIS

During the experimental implementation of impedance spectroscopy and equivalent circuit, it was quite impossible to determine the two processes because they were overlapping with each other, this tool sort the best possible way to clearly show that two processes exist.

### RESULT AND DISCUSSION

Using DRT involves importing electrochemical impedance spectroscopy data into the DRT application from stored EIS data. The first column corresponds to the frequency data, the second and third corresponds to the real and imaginary parts of the EIS data. It is important to note that the frequency data is equally spaced in the logarithm scale to reduce computational effort. After importing, the EIS data was plotted in a complex plot using the DRT tool. This process lasted for a period of 4.4 hours.

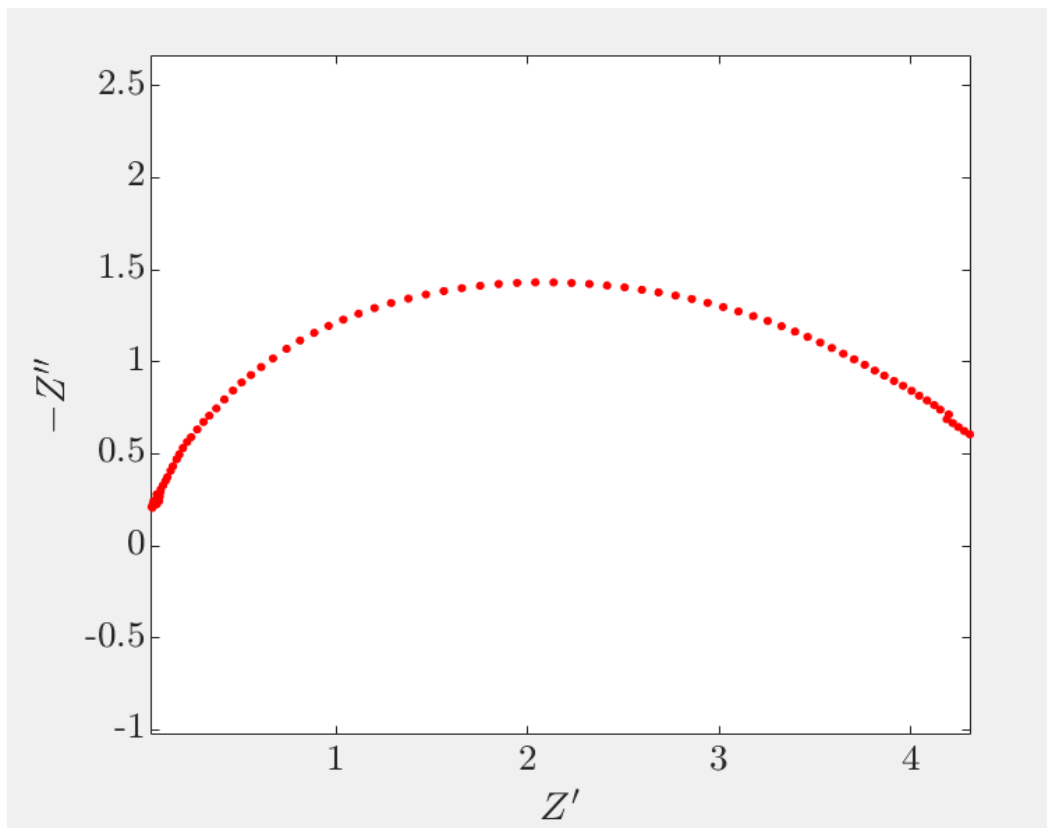


Figure 17: complex plot of EIS DATA



After the importation of the EIS data the regularisation parameter is set to an appropriate scale of 1E-2 and the simple run button is pressed. The regularisation parameter helps to smoothen the DRT profile and stronger the DRT oscillation profile. This can be seen in Figure 18 below.

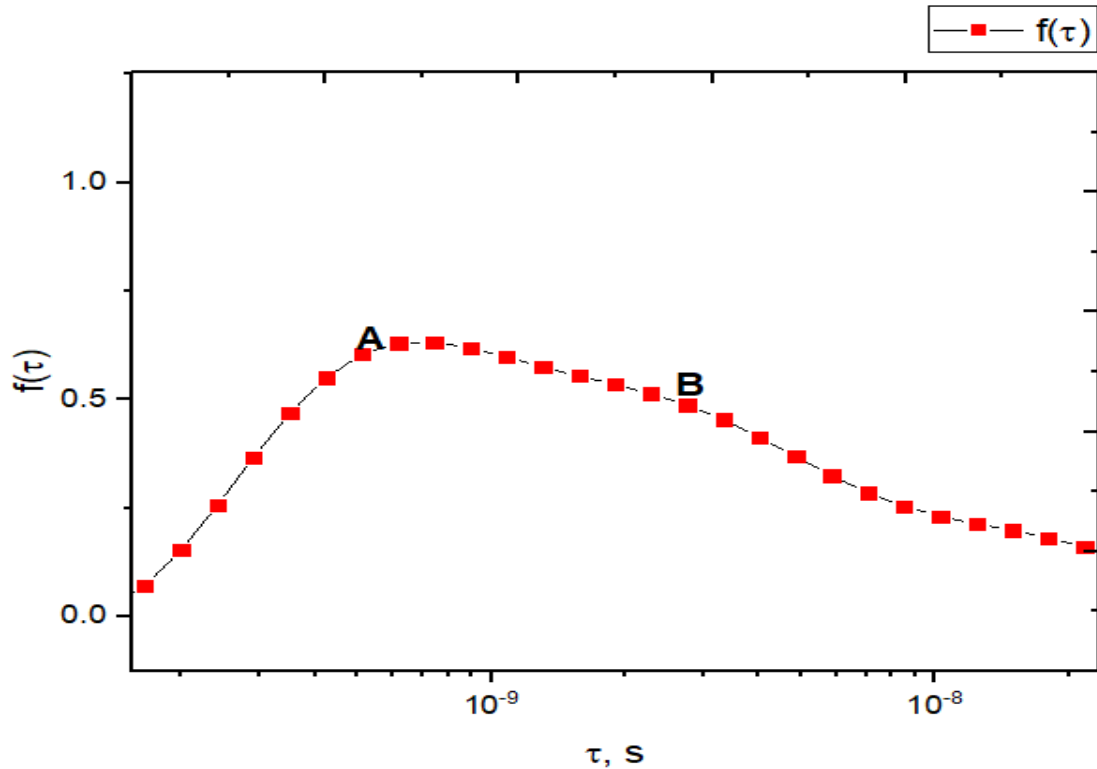


Figure 18: DRT result of the EIS DATA for a period of 4.4 hours.

Figure 17 above is the result of the electrochemical impedance spectroscopy data after the 4.4 hours of crystallisation and its corresponding DRT result (figure 18).

From Figure 18 we can see 2 peaks (A and B) and our forward task will be to fit one Gaussian curve for every DRT peak

## 5. GAUSSIAN FIT OF DRT

It is defined as a continuous fit that calculates the distribution of binomial events in such a way that the values over the distribution gives a probability of [17].

### 5.1 MULTIPLE PEAK FITTING OF DRT

The graphs obtained, is fitted with one gaussian curve for every DRT peak. This process is done using multiple peak fit in origin with the implimentation of the equation below

$$y = Y_0 + \left( \frac{A}{W \cdot \sqrt{\frac{\pi}{2}}} \right) * e^{(-2 * \left( \frac{X - X_C}{W} \right)^2)} \dots \text{formula 6.1}$$

where :  $Y_0$ =base,  $X_C$ =center,  $A$ = Area,

In the beginning of the heat treatment, from the 0 hour, it was just one process which lasted for some time and later assume to become two peaks

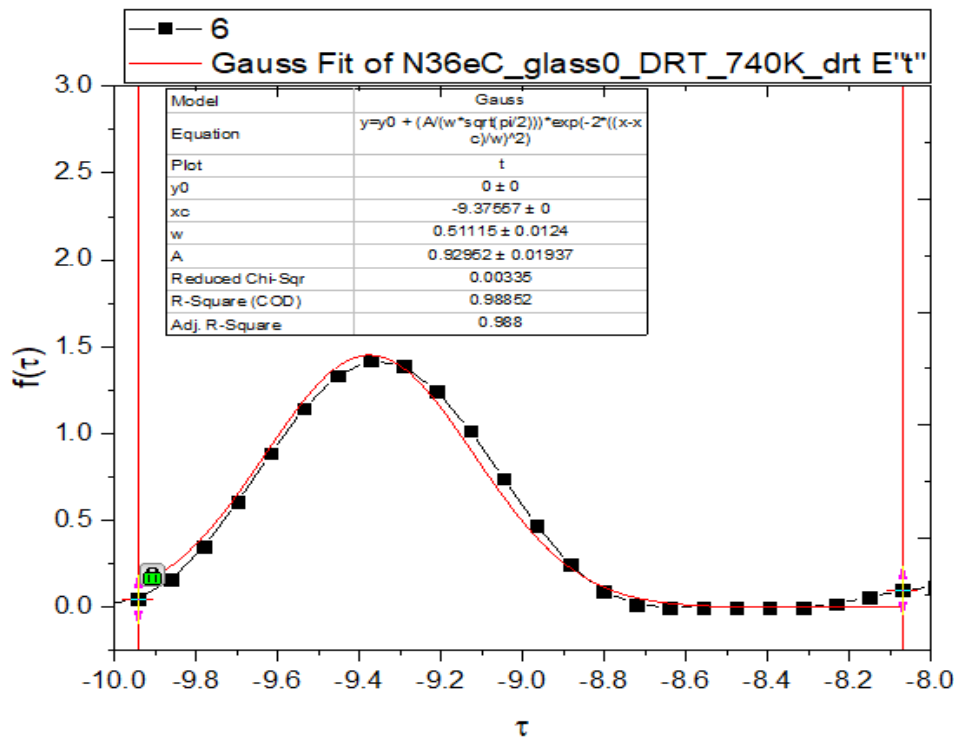


Figure 19: DRT graph from the 0hour and Gaussian fit

From the second phase, ie from 3.5 hours and 4.4 hours of the DRT graph, we noticed two Gaussian fit starts to appear which was confirmed with two different centers as seen in Figure 20&21 below.

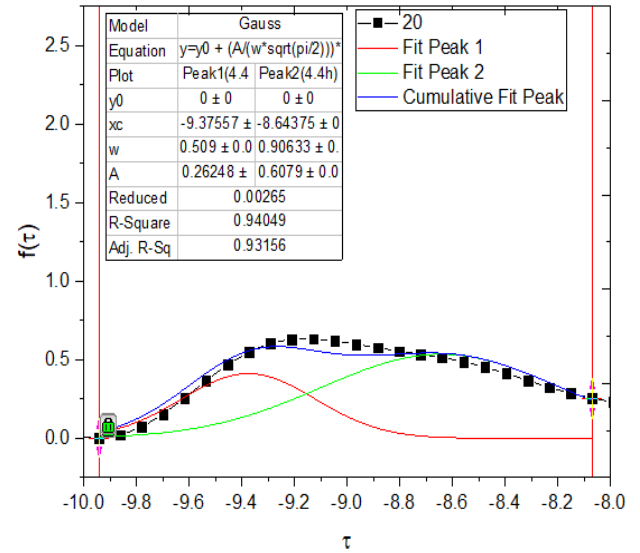
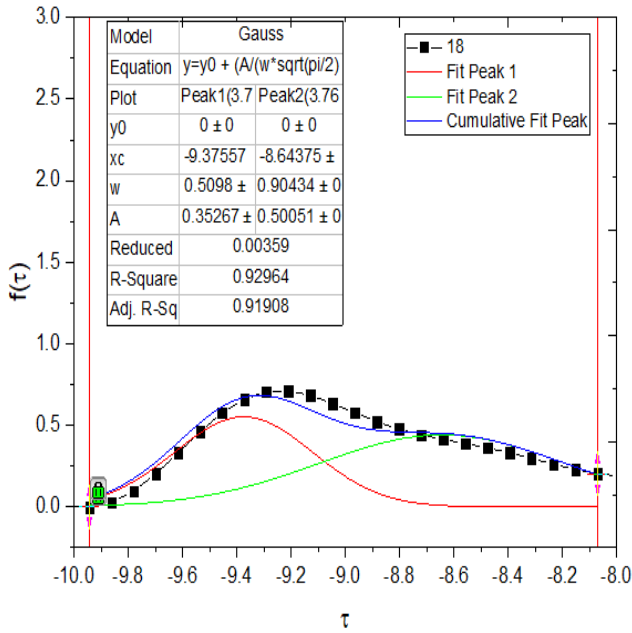


Figure 20: The DRT plot and the Gaussian fit for 3.76h Figure 21: The DRT plot and the Gaussian fit for 4.4h

From the graph above we (Figure 20&21) we can see the appearance of multiple peaks which were not visible in Figure 11 (The Nyquist plot of impedance spectra within 3.76 and 4.4 hours of measurement) using the equivalent circuit method.

From the 5.67 hours, one of the processes began to fade away leaving just one big peak, this is seen in the figures below (Figure 22&23)

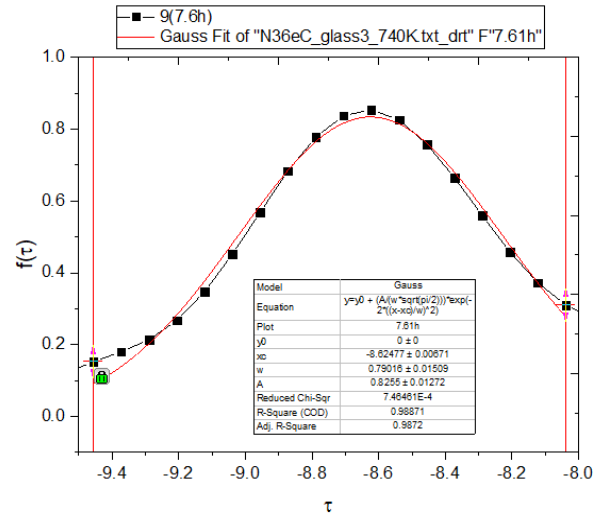
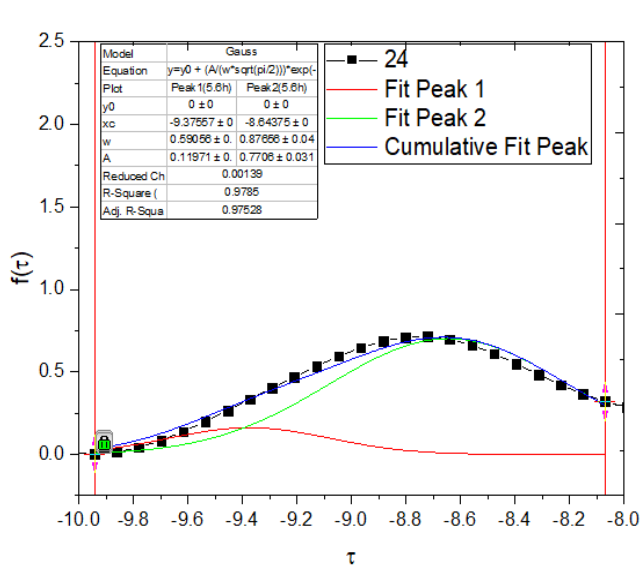


Figure 22: The DRT plot and the Gaussian fit for 5.6h Figure 23: The DRT plot and the Gaussian fit for 7.61h

## 5.2 FITTING IMPEDANCE SPECTRA IN Zview

In order to show that the other side of the graph(far away peaks) does not have any influence on the selected section, the center( $X_c$ ) obtained from the multipeak fitting(Figure 19 to 23) , and other parameters such as the distribution element(DE1 & DE2)(see appendix). Two element of Type-5 in series were used in the Zview application and an equivalent circuit and fitting are done as shown below for all times. The fitting gives the value of the resistance ( $R_1$  &  $R_2$ ). The graphs below represent a Nyquist plot of the crystallization process and the fit from the 0hour of the process.

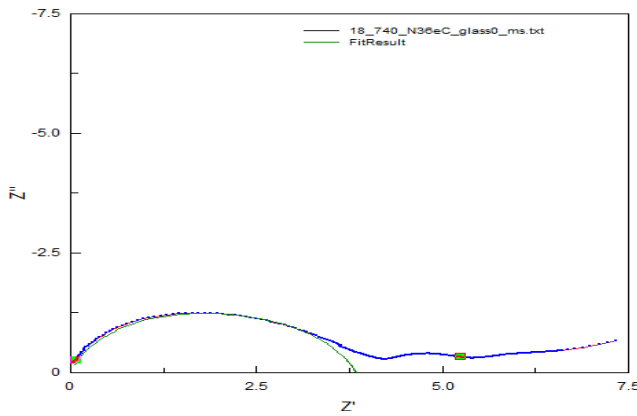


Figure 24: The Nyquist plot and the equivalent circuit fit for the 3.67h

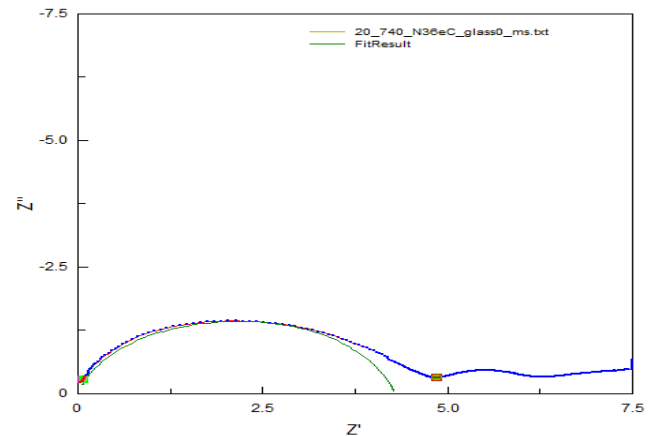


Figure 25: The Nyquist plot and the equivalent circuit fit for the 4.4h

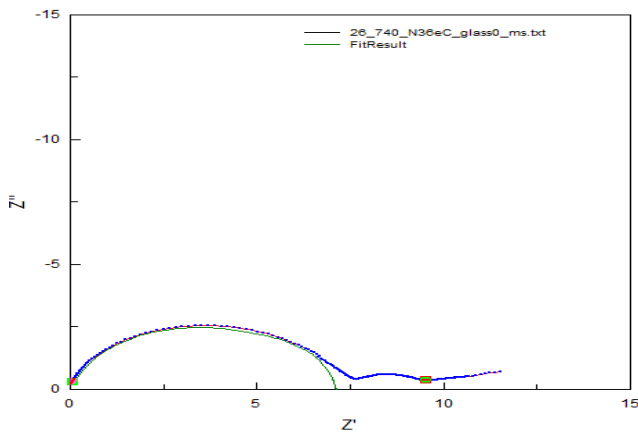


Figure 26: A Nyquist plot and the equivalent circuit fit after 5.67hours

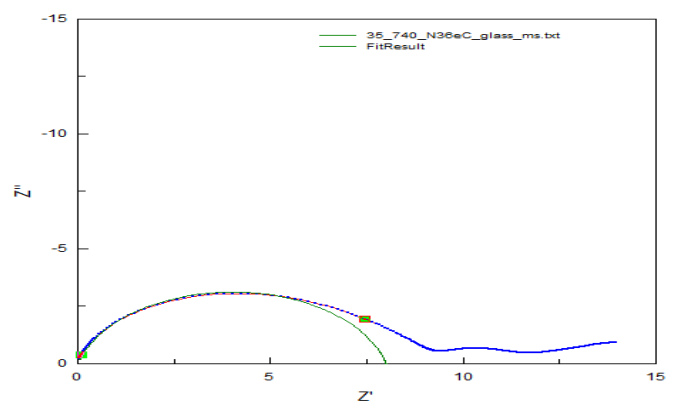


Figure 27: A Nyquist plot and the equivalent circuit fit after 16hours

## RESULTS AND DISCUSSION

The resistances ( $R_1$  &  $R_2$ ) obtained in the equivalent circuit fitting are plotted against time and the ratio ( $\frac{R_2}{R_1}$ ) matched and compared with the area under the Gaussian fit ( $\frac{A_2}{A_1}$ ). From the graphs in Figure 29 below, the value of the ( $\frac{R_2}{R_1}$ ) & ( $\frac{A_2}{A_1}$ ) are compared. As it was established, we try to match the ratio of the area under the graph corresponding to the ratio of the resistance.

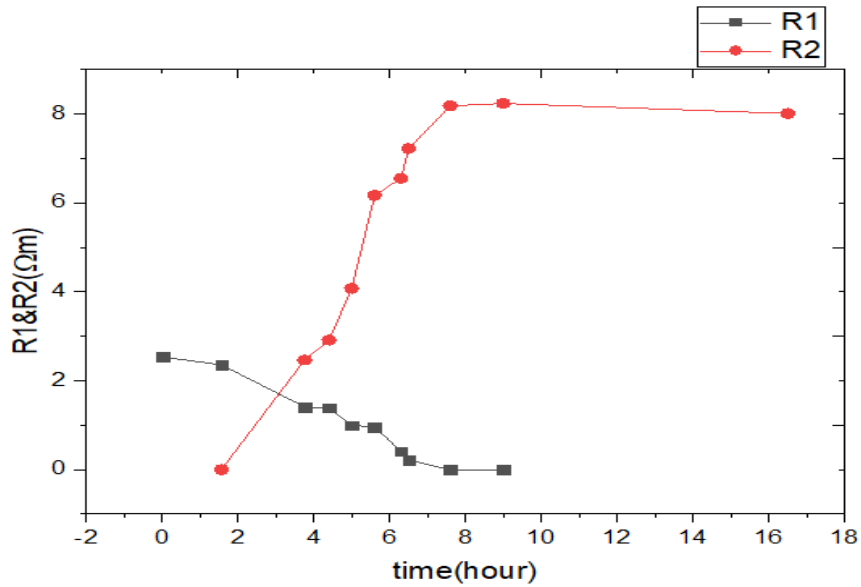


Figure 28: A graph of  $R_1$  &  $R_2$  against time

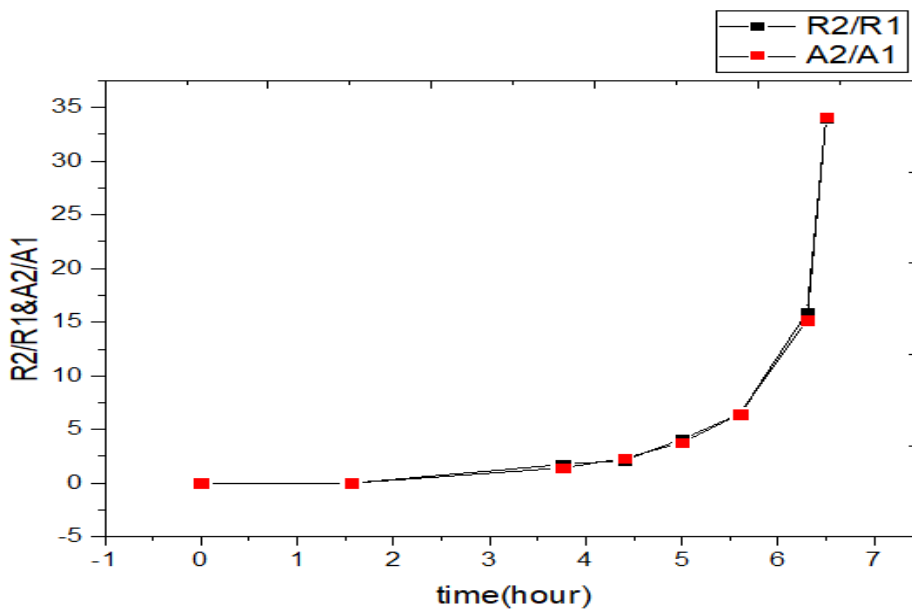


Figure 29: A graph of ratio of  $R_1$  and  $R_2$  against time

## CONCLUSION

We analyze the highest-frequency range in the vicinity of 1GHz and we use the fit of a simple circuit. From our results, we assumed that for glass there is one process and during nanocrystallization, another process appears which is not visible on the bode plots. This issue brings about the introduction of a DRTtool which provides a better resolution of distinct charge relaxation processes than the conventional equivalent circuit(Zview). Fitting one Gaussian curve for every DRT peak gave us a clearer view of the number of peaks present in the process. From the result of the gaussian graphs, we can see the appearance of multiple peaks which were not visible in the Nyquist plot of impedance spectra within 3.76 and 4.4 hours of measurement using the equivalent circuit method. The ratio of resistance obtained from the Zview corresponded to the ratio of area under the gaussian curve.

## SUMMARY

Impedance spectroscopy (IS) is a powerful technique used in applications such as electrochemistry, materials science, biology, medicine, and the semiconductor industry. This technique is based on the interaction of the electric charge of particles inside the sample with an applied electric field and essentially consists in measuring the magnitude of this interaction and its characteristic frequency or time scale. For this experiment,  $\text{Na}_3\text{VTi}(\text{PO}_4)_2\text{F}_3$  glass as the initial sample is held in position with the electrode and the spectrometer was used to provide the electric field through the material and heated at a high temperature of (466.85 degrees Celcius) 740K to nanocrystalise and temperature maintained for 17 hours. During this time nanocrystallization was happening and we were measuring every half an hour impedance of the material, This process is called **in-situ**. The data was collected(33points) and every  $\frac{1}{2}$  an hour and a Bode and Nyquist plot were drawn. A small portion of the graph was considered which is far away as possible in the highest frequency side of the peak from the other side and draw an equivalent circuit. We take the most simple circuit which is R and CPE(not ideal capacitor). During the experimental implementation of impedance spectroscopy using equivalent circuit to analyse the results, it was quite impossible to determine the two processes because they were overlapping with each other. This brought about the DRT(Distribution relaxation time) which sorted the best possible way to clearly show that two processes exist since this method yields a better resolution. To recomfirm that actually two processes occurred we performed gaussian fit of DRT using multipeak fitting and the results obtained clearly showed showed that two processes occurred.

Further more we fitted the impedance spectra in Zview using the center( $X_c$ ) obtained from the multipeak fitting(Figure 19 to 23) , and other parameters such as the distribution element(DE1 & DE2)(see appendix). This was to show that the other side of the graph(far away peaks) does not have any influence on the selected section. Values of the resistances were obtained for all times and The ratio of resistance( $\frac{R_2}{R_1}$ ) obtained from the Zview corresponded to the ratio of area ( $\frac{A_2}{A_1}$ ) under the Gaussian curve(Figure 29 to 31).

### Reference

1. Justyna E. Frąckiewicz, Dominika A. Buchberger, Jerzy E. Garbarczyk . (2021, December 01). Energies. Electrochemical Properties of Pristine and Vanadium Doped LiFePO<sub>4</sub> Nanocrystallized Glasses, p. 14.
2. Tomasz K. Pietrzak, Marek Wasiucioneck, Jerzy E. Garbarczyk . (2021, May 17). Nanomaterials. Towards Higher Electric Conductivity and Wider Phase Stability Range via Nanostructured Glass-Ceramics Processing.
3. Sakamoto, A.; Yamamoto, S. Glass-Ceramics. (2010). Engineering Principles and Applications. application of glass ceramics, 237–247.
4. Pietrzak, T.K.; Wasiucioneck, M.; Michalski, P.P.; Kaleta, A.; Garbarczyk, J.E. (2016). Highly conductive cathode materials for Li-ion batteries are prepared by thermal nanocrystallization of selected oxide glasses. material science engineering, 140–147.
5. Deubener, J.; Allix, M.; Davis, M.J.; Duran, A.; Höche, T.; Honma, T.; Komatsu, T.; Krüger, S.; Mitra, I.; Müller, R.; . (2018). Updated definition of glass ceramics. Nono Crystallisation of Solids , 2-10.
6. Le Meins JM, Crosnier-Lopez MP, Hemon-Ribaud A, Courbion G. (1999). Phase transitions in the Na<sub>3</sub>M<sub>2</sub>(PO<sub>4</sub>)<sub>2</sub>F<sub>3</sub> family (Al<sup>3+</sup>, V<sup>3+</sup>, Fe<sup>3+</sup>, Ga<sup>3+</sup>): synthesis, thermal, structural, and magnetic studies. J Solid State Chem, 148-260.



7. Damour, M.A. (1846). Sur un nouveau phosphate de fer, de manganèse et de soude, l'Alluaudite, trouvé dans le département de la Haute-Vienne. Des Mines , 341–350.
8. Maciej Nowagiel, Algimantas Kežionis, Aldona Zalewska. (2022, April 1). Energies. Electrochemical Performance of Highly Conductive Nanocrystallized Glassy Alluaudite-Type Cathode Materials for NIBs, p. 15.
9. Gleiter, H. (2000). Nanostructured Materials: Basic Concepts and Microstructure. *Advance Mater*, 5-28.
10. Chamryga, A.E.; Nowagiel, M.; Pietrzak, T.K. (2019). Syntheses and nanocrystallization of Na<sub>2</sub>O-M<sub>2</sub>O<sub>3</sub>-P<sub>2</sub>O<sub>5</sub> alluaudite-like phosphate glasses (M = V, Fe, Mn). *NonoCrystallisation of Solids*, 526.
11. Olfa Kanoun, Chemnitz. (2019). Impedance Spectroscopy. De Gruyter.
12. F. Kremer, A. Schonhal. (2012). Broadband Dielectric Spectroscopy. Springer Science & Business Media, 729.
13. Robert S. Eisenberg, C. M. Roland, Norbert Wagner, et al. (2018, march 25). Impedance Spectroscopy: Theory, Experiment, and Applications. Retrieved from onlinelibrary.wiley.com: <https://onlinelibrary.wiley.com/>
14. G. J. Brug, A. L. G. van den Eeden, M. Sluyters-Rehbach, J. H. Sluyters. (1984). The analysis of electrode impedances is complicated by the presence of a constant phase element. *Electroanalysis Chem.*, 275-295.
15. A. Kežionis, E. Kazakevičius, Some features of the analysis of broadband impedance data using the distribution of relaxation times, *Electrochim. Acta* 349 (2020) 136379, <https://doi.org/10.1016/j.electacta.2020.136379>.
16. H. Schichlein, A.C. Muller, M. Voigts, A. Krugel, Ivers-Tiffée, Deconvolution of electrochemical impedance spectra for the identification of electrode reaction mechanisms in solid oxide fuel cells, *E., J. Appl. Electrochem.* 32 (2002) 875e882, <https://doi.org/10.1023/A:1020599525160>.
17. T.H. Wan, M. Saccoccio, C. Chen, F. Ciucci. (2015). Influence of the Discretization Methods on the Distribution of Relaxation Times Deconvolution. Retrieved from Implementing Radial Basis Functions with DRTtools,.: [doi.org/10.1016/j.electacta.2015.09.097](https://doi.org/10.1016/j.electacta.2015.09.097)
18. Equivalent Circuits - Distributed Elements, 1990-2007 scibner associates, Inc. written by Derek Johnson

## APPENDIX: DISTRIBUTED ELEMENT(DE)

A Distributed element (DE) can be inserted anywhere in a circuit model. Each Distributed Element (DE) is defined by 5 main parameters; **R**, **DE-Type**, **T**, **U**, and **P**. The Extended Distributed Elements (DX) are distributed elements that require more than 5 parameters to define their values. In addition to the Type, **DX-Type**, **R**, **T**, **U**, and **P** values, **A** and **B** parameters are also used. The DE-Type value selects which distributed element type is to be used. In the following pages, each element is listed according to its DE-Type value. If DE-Type=0 the DE is not used, independent of the values for the other DE parameters. R, T, U, and P are free parameters that have different values for each type of DE. They usually use the following convention[18]:

- R - Usually resistance
- T - A time constant or capacitance.
- U - Usually a resistance or an exponent
- P - An exponent

Note: When DE-Type is set to negative, a special option is available. In this case, DE returns the resistance of the dielectric element, calculated from the calculated value of the function (where R is taken as  $C_{zero} - C_{inf}$ ) as a complex dielectric constant (or capacitance) and converted to resistance. Specifically, if this option is selected, the function takes the calculated "impedance" of the element, then takes the return value and divides it by

$$I * C_{zero} * w.$$

$$Z_{diel} = \left( \frac{1}{I * C_{zero} * w * Z} \right)$$

See the discussion in the paper by MacDonald and Potter--Solid State Ionics. In addition to the various distributed elements, there are two simple varieties of discrete circuits (DE-Type = 1 and 17). These allow more flexibility in the model circuits.

**Select a DE-Type from the following list:**

- Type 0 - Short Circuit==DE\_0}
- Type 1 - RC Parallel Combination==DE\_1}
- Type 2,3 - Constant Phase Element (CPE) and/or Series RC==DE\_2}
- Type 4,5 - ZARC-Cole Element==DE\_4}
- Type 6,7,8 - Havriliak-Nagami Element==DE\_6}
- Type 9 - Generalized Finite Warburg Element==DE\_9}
- Type 10 - Williams-Watts Fractional Exponential==DE\_10}
- Type 11 - Jonsher Response==DE\_11}
- Type 12 - Exponential Distribution of Activation Energies (Form1)==DE\_12}
- Type 13 - Exponential Distribution of Activation Energies (Form2)==DE\_13}
- Type 14 - Gaussian Distribution of Activation Energies==DE\_14}
- Type 15,16 - General Diffusion DCE==DE\_15}

Type 17 - Ideal RCL Elements==DE\_17}